Report

Cell Reports

Enteroendocrine Cells Support Intestinal Stem-Cell-Mediated Homeostasis in *Drosophila*

Graphical Abstract

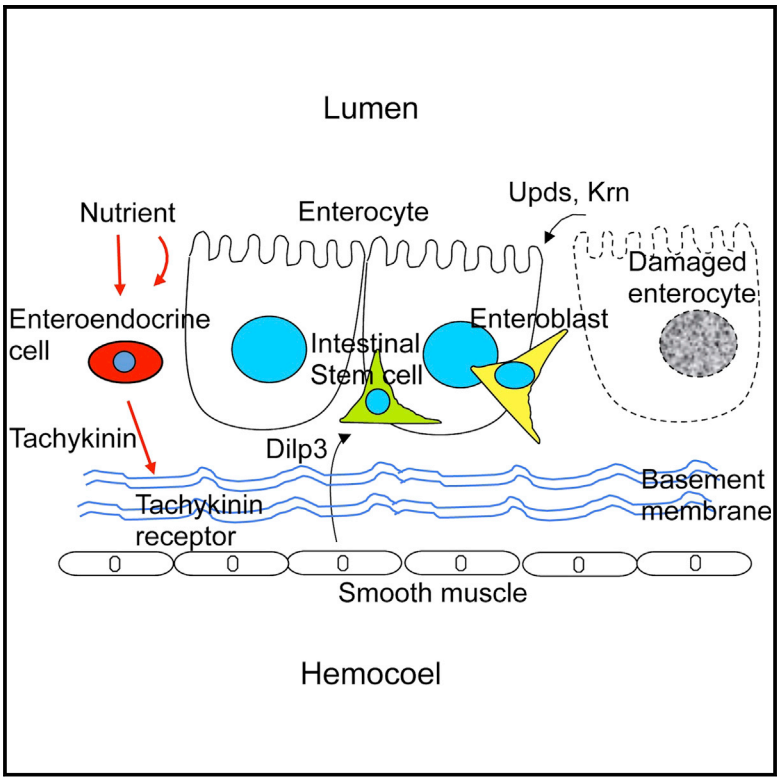

Highlights

The *AS-C* gene *scute* is necessary for the development of enteroendocrine cells

Enteroendocrine cells support nutrient-stimulated intestinal stem cell division

Tachykinin is a gut hormone mediating the enteroendocrine cell-regulated growth

Tachykinin regulates DILP3 expression in visceral muscle for intestinal growth

Authors

Alla Amcheslavsky, Wei Song, ..., Norbert Perrimon, Y. Tony Ip

Correspondence

tony.ip@umassmed.edu

In Brief

Amcheslavsky et al. show that enteroendocrine cells serve a niche function to regulate intestinal stem cell division. High-nutrient diet stimulates intestinal stem cell division and intestinal tissue growth in newly eclosed flies. Enteroendocrine cells act as an important link for this process by producing gut hormones such as Tachykinin to regulate the expression of an insulin-like peptide DILP3 in the visceral muscle. This *Drosophila* model helps to elucidate the function of enteroendocrine cells in complex whole-animal physiology.

Amcheslavsky et al., 2014, Cell Reports 9, 32–39
October 9, 2014 ©2014 The Authors
http://dx.doi.org/10.1016/j.celrep.2014.08.052

OPEN ACCESS
CellPress

Cell Reports
Report

Enteroendocrine Cells Support Intestinal Stem-Cell-Mediated Homeostasis in *Drosophila*

Alla Amcheslavsky,[1] Wei Song,[2,3] Qi Li,[1] Yingchao Nie,[1] Ivan Bragatto,[4] Dominique Ferrandon,[4] Norbert Perrimon,[2,3] and Y. Tony Ip[1,*]
[1]Program in Molecular Medicine, University of Massachusetts Medical School, Worcester, MA 01605, USA
[2]Howard Hughes Medical Institute, Harvard Medical School, Boston, MA 02115, USA
[3]Department of Genetics,Harvard Medical School, Boston, MA 02115, USA
[4]Unité Propre de Recherche 9022 du Centre National de la Recherche Scientifique, University of Strasbourg Institute for Advanced Study, Institut de Biologie Moléculaire et Cellulaire, 67084 Strasbourg Cedex, France
*Correspondence: tony.ip@umassmed.edu
http://dx.doi.org/10.1016/j.celrep.2014.08.052

SUMMARY

Intestinal stem cells in the adult *Drosophila* midgut are regulated by growth factors produced from the surrounding niche cells including enterocytes and visceral muscle. The role of the other major cell type, the secretory enteroendocrine cells, in regulating intestinal stem cells remains unclear. We show here that newly eclosed *scute* loss-of-function mutant flies are completely devoid of enteroendocrine cells. These enteroendocrine cell-less flies have normal ingestion and fecundity but shorter lifespan. Moreover, in these newly eclosed mutant flies, the diet-stimulated midgut growth that depends on the insulin-like peptide 3 expression in the surrounding muscle is defective. The depletion of Tachykinin-producing enteroendocrine cells or knockdown of *Tachykinin* leads to a similar although less severe phenotype. These results establish that enteroendocrine cells serve as an important link between diet and visceral muscle expression of an insulin-like growth factor to stimulate intestinal stem cell proliferation and tissue growth.

INTRODUCTION

The gastrointestinal (GI) tract is a complex organ essential for nutrient absorption and whole-body metabolism (Miguel-Aliaga, 2012). The *Drosophila* midgut is an equivalent of the mammalian stomach and small intestine. The midgut epithelium has no crypt-villus structure but instead is a monolayer of absorptive enterocytes (ECs), with interspersed intestinal stem cells (ISCs), enteroblasts (EBs), and enteroendocrine cells (EEs) located closer to the basement membrane (Micchelli and Perrimon, 2006; Ohlstein and Spradling, 2006).

All cells in the midgut likely constitute together the niche that regulates ISC proliferation and EB differentiation for tissue homeostasis. The visceral muscle secretes Wingless, insulin-like peptides, epidermal growth factor receptor (EGFR) ligands, and Decapentaplegic (Dpp)/bone morphogenetic protein (Guo et al., 2013; Jiang et al., 2011; Lin et al., 2008; O'Brien et al., 2011). The mature ECs are a major source of stress-induced Dpp, EGFR ligands, and the JAK-STAT pathway ligands Unpaired (Upd) 1–3 (Biteau and Jasper, 2011; Buchon et al., 2010; Guo et al., 2013; Jiang et al., 2009, 2011; Li et al., 2013a; Osman et al., 2012; Tian and Jiang, 2014; Xu et al., 2011). The differentiating EBs also produce Upds, Wingless, and EGFR ligands (Cordero et al., 2012; Jiang et al., 2011; Zhou et al., 2013). The surrounding trachea secretes Dpp, while the innervating neurons can also regulate intestinal physiology (Cognigni et al., 2011; Li et al., 2013b).

EEs constitute a major cell type in the *Drosophila* midgut epithelium. While the mammalian secretory lineage is differentiated into Paneth cells, goblet cells, enteroendocrine cells, and tuft cells (Gerbe et al., 2012), the entire population of secretory cells in the *Drosophila* midgut is collectively called EEs and marked by the homeodomain protein Prospero (Pros) (Micchelli and Perrimon, 2006). Nonetheless, different subsets of hormones are produced from different subtypes of midgut EEs (Ohlstein and Spradling, 2006). In the mouse intestine, the Lgr5+ ISCs directly contact Paneth cells, and isolated ISC-Paneth cell doublets have higher efficiency to form organoids (Sato et al., 2011). However, mouse genetic knockout that has Paneth cells removed did not result in the loss of Lgr5+ ISCs (Durand et al., 2012). Only recently have *Drosophila* midgut EEs been shown to negatively regulate ISC proliferation via EGFR ligand production and to regulate ISC differentiation via the Slit/Robo pathway (Biteau and Jasper, 2014; Scopelliti et al., 2014). Therefore, the function of EEs in regulating stem cell activity largely remains to be investigated. Here, we show that *Drosophila* midgut EEs serve a niche function by producing hormones such as Tachykinin (Tk) to regulate insulin peptide expression in the surrounding muscle that in turn affects intestinal homeostasis.

RESULTS AND DISCUSSION

scute RNAi and Deletion Result in EE-less Flies

Previous evidence shows that adult midgut mutant clones that have all the *AS-C* genes deleted are defective in EE formation while overexpression of *scute* (*sc*) or *asense* (*ase*) is sufficient

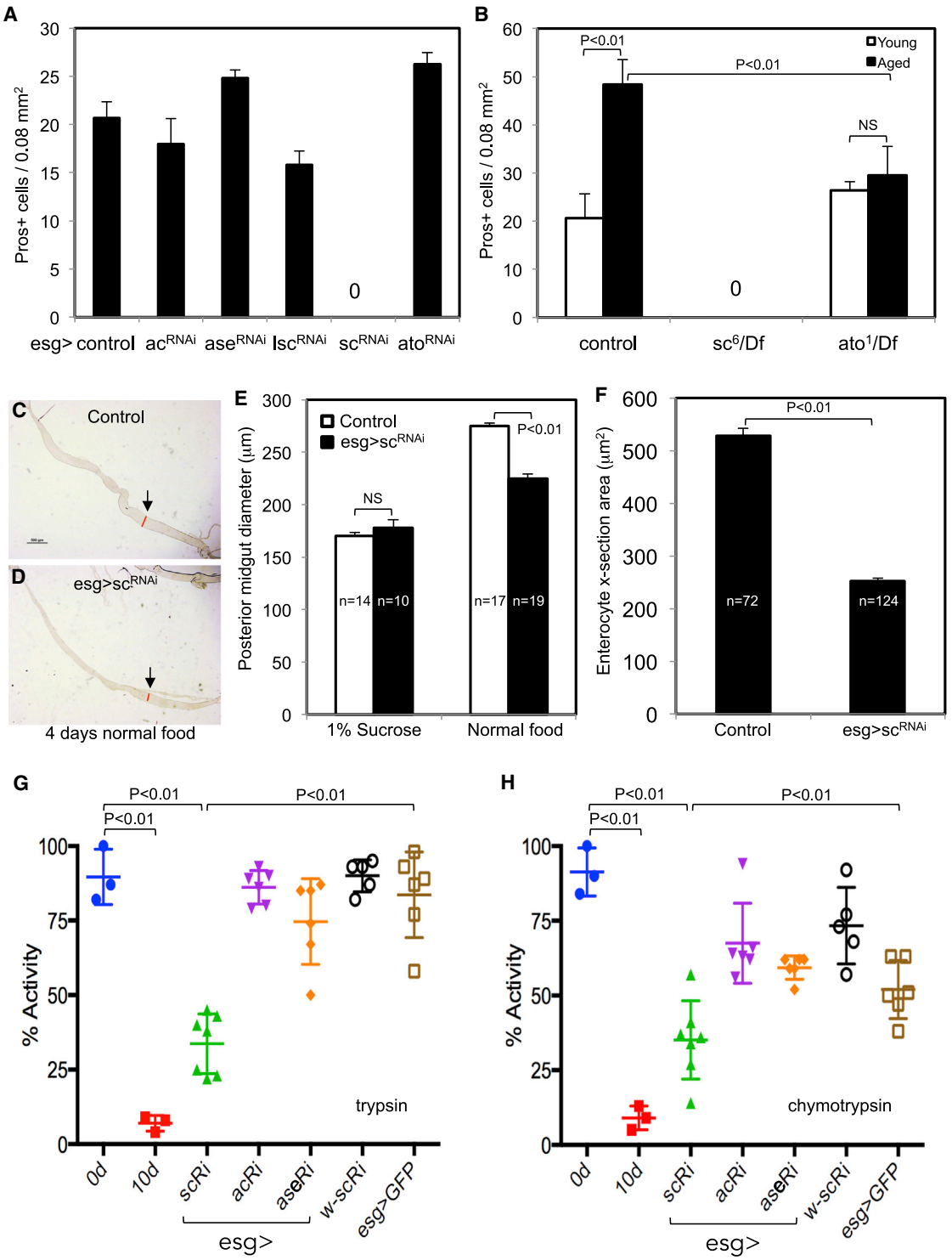

Figure 1. EE-less Fly Guts after Loss of *sc* Function Have Growth Defects

(A) The number of Pros+ nuclei was counted within 0.08 mm^2 surface area of a microscopic image from a similar region of each posterior midgut. The sc^{RNAi} midguts were completely devoid of EEs.

(B) EE quantification in the midguts of flies with the genotypes indicated. Control was *w-*, and the deficiency for *sc* was $Df(1)sc^{10-1}$ and for *ato* was *Df(3R)p13*. Young flies were 7 days old, and aged flies were 21 days old. NS, nonsignificant ($p > 0.05$), and all p values are from the Student's t test.

(C and D) Light microscope images of control and esg > sc^{RNAi} fly midguts. The arrow and hair line point to the posterior midgut region where images were taken to measure the diameter.

(legend continued on next page)

to increase EE formation (Bardin et al., 2010). Moreover, the Notch pathway with a downstream requirement of *ase* also regulates EE differentiation (Micchelli and Perrimon, 2006; Takashima et al., 2011; Zeng et al., 2013). To study the requirement of EEs in midgut homeostasis, we first attempted to delete all EEs by knocking down each of the *AS-C* transcripts using the ISC/EB driver esg-Gal4. The results show that *sc* RNAi was the only one that caused the loss of all EEs in the adult midgut (Figures 1A and S1A–S1F). The esg-Gal4 driver is expressed in both larval and adult midguts, but the esg > *sc* RNAi larvae were normal while the newly eclosed adults had no EEs. Therefore, *sc* is likely required for all EE formation during metamorphosis when the adult midgut epithelium is reformed from precursors/stem cells (Jiang and Edgar, 2009; Micchelli et al., 2011).

The $sc^{6}/sc^{10\text{-}1}$ hemizygous mutant adults were also completely devoid of midgut EEs (Figures 1B, S1G, and S1H), while other hemizygous combinations including sc^{1}, sc^{3B}, and sc^{5} were normal in terms of EE number. $Df(1)sc^{10\text{-}1}$ is a small deficiency that has both *ac* and *sc* uncovered. sc^{1} and sc^{3B} each contain a gypsy insertion in far-upstream regions of *sc*, while sc^{5} and sc^{6} are 1.3 and 17.4 kb deletions, respectively, in the *sc* 3′ regulatory region (García-Bellido and de Celis, 2009). The $sc^{6}/sc^{10\text{-}1}$ combination may affect *sc* expression during midgut metamorphosis and thus the formation of all adult EEs.

The atonal homolog 1 (Atoh1) is required for all secretory cell differentiation in mouse (Durand et al., 2012; VanDussen and Samuelson, 2010). However, esg-Gal4-driven *atonal* (*ato*) RNAi and the amorphic combination $ato^{1}/Df(3R)p13$ showed normal EE formation (Figures 1A, 1B, S1F, S1I, and S1J). Nonetheless, we found that older $ato^{1}/Df(3R)p13$ flies exhibited a significantly lower increase of EE number (Figure 1B), suggesting a role of *ato* in EE differentiation in adult flies.

Changing the Number of EEs Alters Lifespan

In *sc* RNAi guts, the mRNA expression of allatostatin (Ast), allatostatin C (AstC), Tachykinin (Tk), diuretic hormone (DH31), and neuropeptide F (NPF) was almost abolished (Figure S1K), consistent with the absence of all EEs. On the other hand, the mRNA expression of the same peptide genes in heads showed no significant change (Figure S1L). Even though the EEs and regulatory peptides were absent from the midgut, the flies were viable and showed no apparent morphological defects. There was no significant difference in the number of eggs laid and the number of pupae formed from control and *sc* RNAi flies (Figure S1M), suggesting that the flies probably have sufficient nutrient uptake to support the major physiological task of reproduction. However, when we examined the longevity of these animals, the EE-less flies after *sc* RNAi showed significantly shorter lifespan (Figure S1N). In addition, when the number of EEs was increased in adult flies by esgGal4; $tubGal80^{ts}$ (esg^{ts} >)-driven *sc* overexpression (Bardin et al., 2010; Figure S3), an even shorter lifespan was observed. These results suggest that a balanced number of EEs is essential for the long-term health of the animal. Moreover, there may be important physiological changes in these EE-less flies that are yet to be uncovered, such as reduced intestinal growth described in detail below.

EE-less Flies Have Reduced Intestinal Growth as Observed under Starvation Conditions

One of the phenotypic changes we found for the *sc* RNAi/EE-less flies was that under normal feeding conditions, their midguts had a significantly narrower diameter than that of control midguts (Figures 1C and 1D). When reared in poor nutrition of 1% sucrose, both wild-type (WT) and EE-less flies had thinner midguts. When reared in normal food, WT flies had substantially bigger midgut diameter, while EE-less flies had grown significantly less (Figure 1E). The cross-section area of enterocytes in the EE-less midguts was smaller (Figure 1F), suggesting that there is also a growth defect at the individual cell level.

A series of experiments showed that ingestion of food dye by the *sc* RNAi/EE-less flies was not lower than control flies (Figure S2C). The measurement of food intake by optical density (OD) of gut dye contents also showed similar ingestion (Figure S2D). The measurement of excretion by counting colored deposits and visual examination of dye clearing from guts showed that there was no significant change in food passage (Figures S2E and S2F). The normal fecundity shown in Figure S1M also suggested that the mutant flies likely had absorbed sufficient nutrient for reproduction. Nonetheless, another phenotype we could detect was a substantial reduction of intestinal digestive enzyme activities including trypsin, chymotrypsin, aminopeptidase, and acetate esterase (Figures 1G, 1H, S2A, and S2B). These enzyme activities exhibit strong reduction after starvation of WT flies. The EE-less flies therefore have a physiological response as if they experience starvation although they are provided with a normal diet.

EE-less Midguts Have Reduced ISC Division and Dilp3 Expression

A previous report has established that newly eclosed flies respond to nutrient availability by increasing ISC division that leads to a jump start of intestinal growth (O'Brien et al., 2011). When we fed newly eclosed flies on the poor diet of 1% sucrose, both WT and *sc* RNAi/EE-less guts had a very low number of p-H3-positive cells (Figure 2A), which represent mitotic ISCs because ISCs are the only dividing cells in the adult midgut. When fed on normal diet, the WT guts had significantly higher p-H3 counts, but the *sc* RNAi/EE-less guts were consistently lower at all the time points. The $sc^{6}/sc^{10\text{-}1}$ hemizygous mutant combination exhibited a similarly lower mitotic activity on the normal diet (Figure 2B).

(E) Quantification of the diameter of the midguts after the starving (1% sucrose) or normal feeding condition.
(F) The cross-section area of each enterocyte based on confocal images of Armadillo staining that outlined the cell shape was measured, and the average is plotted as shown.
(G and H) Midguts from fertilized females (7–10 days old) were homogenized and used for enzymatic assay. Each genotype corresponded to five to six samples of ten midguts each. The sample with the highest activity in each enzyme assay was set as 100%, and all others were calculated as a fraction.
Data are presented as mean ± SEM (error bar).

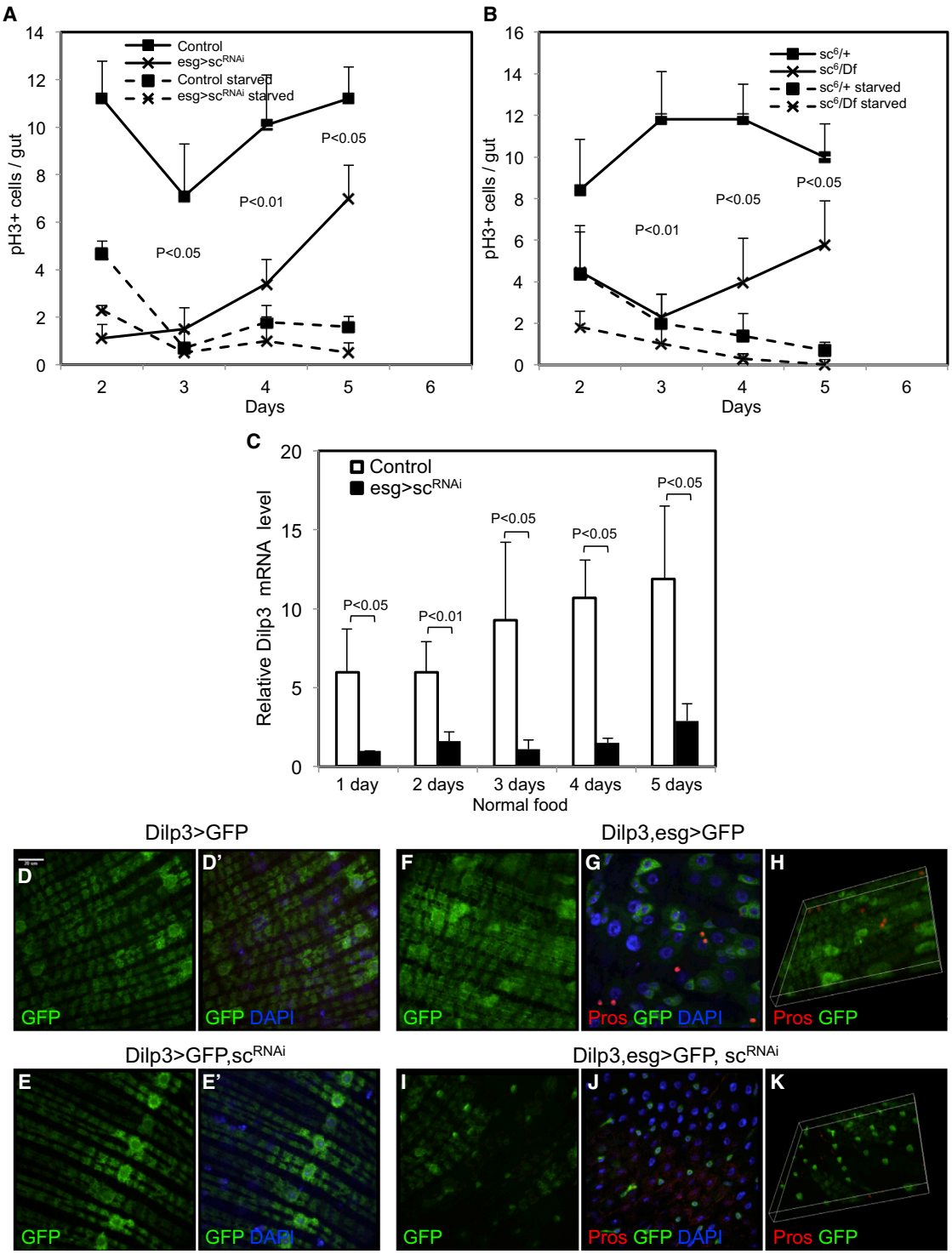

Figure 2. EE-less Guts Have ISC Proliferation and *Dilp3* Expression Defects

(A and B) Newly hatched flies (day 1) were collected and kept in normal food vials or plastic vials with filter paper soaked with 1% sucrose (starved). Each day after, midguts were dissected from flies of the indicated genotypes and stained for p-H3 to detect mitotic cells. Average number of p-H3+ cells is plotted as shown. The esg > GFP in (A) or *sc*/+ in (B) served as controls. The deficiency is *Df(1)sc*$^{10\text{-}1}$.

(C) *Dilp3* mRNA expression assayed by qPCR. Newly hatched esg > GFP (control) and esg > GFP, *sc*^{RNAi} flies were kept in normal food vials for 1 to 5 days as indicated. At each indicated day, ten flies from each sample were used for gut dissection, RNA isolation, and qPCR. Each qPCR cycle number of *Dilp3* was

(legend continued on next page)

When we investigated possible signaling defects in the EE-less flies, we found that in addition to other gut peptide mRNAs, the level of *Dilp3* mRNA was also highly decreased in these guts while the head *Dilp3* was normal (Figures 2C and S1L). This is somewhat surprising, because *Dilp3* is expressed not in the epithelium or EEs but in the surrounding muscle (O'Brien et al., 2011; Veenstra et al., 2008). We used *Dilp3* promoter-Gal4-driven upstream activating sequence (UAS)-GFP expression (Dilp3 > GFP) to visualize the expression in muscle (Figure 2D). Both control and *sc* RNAi under this driver showed normal muscle GFP expression (Figure 2E), demonstrating that *sc* does not function within the smooth muscle to regulate *Dilp3* expression. We then combined the esg-Gal4 and Dilp3-Gal4, and the control UAS-GFP samples showed the expected expression in both midgut precursors and surrounding muscles (Figures 2F–2H). When these combined Gal4 drivers were used to drive *sc* RNAi, the smooth muscle GFP signal was clearly reduced (Figures 2I–2K). These guts also exhibited no Prospero staining and overall fewer cells with small sizes as expected from esg > *sc* RNAi (Figures 2I–2K).

The report by O'Brien et al. (2011) showed an increase of *Dilp3* expression from the surrounding muscle in newly eclosed flies under a well-fed diet (see also Figure 2C). This muscle *Dilp3* expression precedes brain expression and is essential for the initial nutrient stimulated intestinal growth. Our EE-less flies show similar growth and *Dilp3* expression defects, suggesting that EE is a link between nutrient sensing and *Dilp3* expression during this early growth phase.

Increasing the Number of EEs Promotes ISC Division Partly via Dilp3 Expression

WT and *AS-C* deletion (sc^{B57}) mutant clones in adult midguts did not exhibit a difference in their cell numbers (Bardin et al., 2010). Moreover, we performed esg^{ts} > *sc* RNAi in adult flies for 3 days but did not observe a decrease of mitotic count or EE number. Together, these results suggest that *sc* is not required directly in ISC for proliferation, and they imply that the ISC division defects observed in the *sc* mutant/EE-less flies is likely due to the loss of EEs. To investigate this idea further, we used the esg^{ts} > system to up- and downshift the expression of *sc* at various time points and measure the correlation of *sc* expression, EE number, and ISC mitotic activity. The overexpression of *sc* after shifting to 29°C for a few days correlated with increased EE number, expression of gut peptides, and increased ISC activity (Figure S3A–S3I). Then, we downshifted back to room temperature (23°C) to allow the $Gal80^{ts}$ repressor to function again. The *sc* mRNA expression was quickly reduced within 2 days and remained low for 4 days (Figure 3A). Although we did not have a working antibody to check the Sc protein stability, the expression of a probable downstream gene *phyllopod* (Reeves and Posakony, 2005) showed the same up- and downregulation (Figure 3B), revealing that Sc function returned to normal after the temperature downshift. Meanwhile, the number of Pros+ cells and p-H3 count remained higher after the downshift (Figures 3C and 3D). Therefore, the number of EEs, but not *sc* mRNA or function, correlates with ISC mitotic activity.

We performed another experiment that was independent of *sc* expression or expression in ISCs. The antiapoptotic protein p35 was driven by the pros-Gal4 driver, which is expressed in a subset of EEs in the middle and posterior midgut (Figures S4B–S4E). This resulted in a significant albeit smaller increase in EE number and a concomitant increase in mitotic activity (Figures S3J and S3K), which was counted only in the middle and posterior midgut due to some EC expression of this driver in the anterior region (Figure S4C). Therefore, the different approaches show consistent correlation between EE number and ISC division.

Dilp3 expression was significantly although modestly increased in flies that had increased EE number after *sc* overexpression (Figure 3E), similar to that observed in fed versus fasted flies (O'Brien et al., 2011). We tested whether *Dilp3* was functionally important in this EE-driven mitotic activity. Due to the lethality, we could not obtain a fly strain that had esg-Gal4, Dilp3-Gal4, UAS-Dilp3RNAi, tub-Gal80ts, and UAS-sc to perform a comparable experiment as shown in Figure 2. So instead, we generated flies that contained a ubiquitous driver with temperature controlled expression, i.e., tub-$Gal80^{ts}$/UAS-sc; tub-Gal4/UAS-Dilp3RNAi. These fly guts showed a significantly lower number of p-H3+ cells than that in the tub-$Gal80^{ts}$/UAS-sc; tub-Gal4/+ control flies (Figure 3F). These results demonstrate that the EE-regulated ISC division is partly dependent on *Dilp3*. The expression of an activated insulin receptor by esg-Gal4 could highly increase midgut proliferation, and this effect was dominant over the loss of EEs after sc^{RNAi} (Figure S4A), which is consistent with an important function of insulin signaling in the midgut.

Tk-Secreting EEs Have a Role in Regulating Dilp3 and ISC Proliferation

As stated above, normally hatched flies did not lower their EE number after esg^{ts} > *sc* RNAi, perhaps due to redundant function with other basic-helix-loop-helix proteins in adults. The expression of proapoptotic proteins by the $pros^{ts}$-Gal4 also could not reduce the EE number. We thus screened other drivers and identified a *Tk* promoter Gal4 (Tk-Gal4) that had expression recapitulating the Tk staining pattern representing a subset of EEs (Figures S4B and S4F–S4I″). More importantly, when used to express the proapoptotic protein Reaper (Rpr), this driver caused a significant reduction in the EE number (Figure S4J),

normalized with that of *rp49* in a parallel reaction of the same RNA sample. The lowest *Dilp3* expressing sample esg > sc^{RNAi} at day 1 was set as 1 (first black bar), and all other samples were calculated as relative level and plotted as shown.

(D and E) *Dilp3* promoter-Gal4 driven UAS-GFP expression (Dilp3 > GFP) illuminates the smooth muscle surrounding the adult midgut epithelium. This expression of muscle Dilp3 > GFP is not altered when the UAS-sc^{RNAi} construct is also driven by this *Dilp3* promoter.

(F–K) Confocal images of midgut at an outer focal plane showing the visceral muscle staining, an inner focal plane showing the epithelium staining and 3D reconstruction of multiple focal planes. The control flies contained the combination of esg-Gal4 and Dilp3-Gal4 together driving UAS-GFP expression. The bottom panels (I–K) were from a fly strain that also contained the sc^{RNAi} construct.

Data are presented as mean ± SEM (error bar).

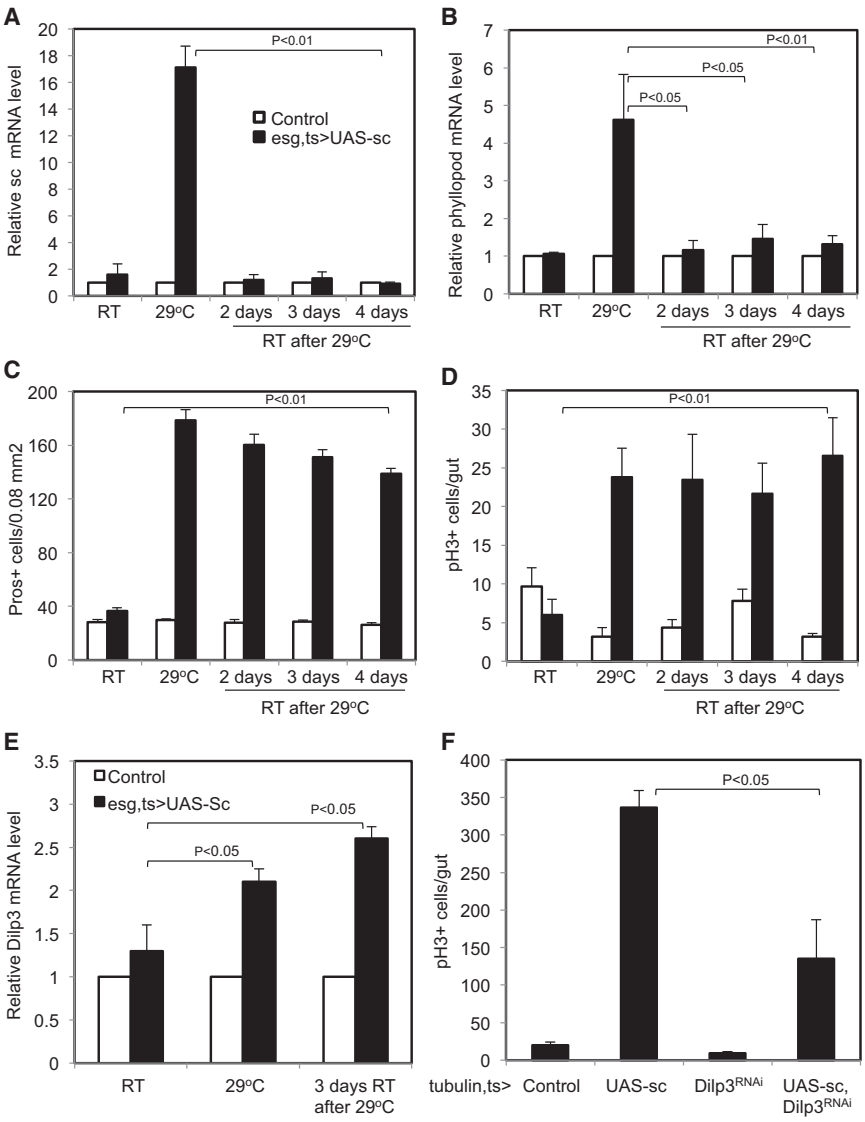

Figure 3. Increasing the Number of EEs Promotes ISC Division Partly via Dilp3

(A–D) Downshift experiments were performed by placing the esgGal4-tubulinGal80^{ts} (esg^{ts} >) flies first at 29°C for 3 days and then back to room temperature (approximately 23°C). On the indicated days, fly guts were dissected to use for *sc* mRNA and *phyllopod* mRNA PCR assays. Each *sc* and *phyllopod* PCR cycle number was normalized with that of *rp49*, and the normalized control sample at each time point was set as 1, and the normalized UAS-sc sample of the same time point was calculated as fold change over the control. Equal numbers of flies from the same vials were used separately for Pros and p-H3 staining and quantification.

(E) Three-day-old flies kept at room temperature with the genotype esg^{ts} > GFP (control) and esg^{ts} > GFP,UAS-sc were shifted to 29°C for 3 days and then shifted back to room temperature for additional 3 days. The normalized *Dilp3* mRNA of control at each time point was set as 1 and that of the UAS-sc of the same time point was calculated as fold change.

(F) The tubulin-Gal4 driver with the temperature-sensitive repressor tubulinGal80^{ts} (tubulin, ts >) were crossed together with the transgenic constructs UAS-GFP as control, UAS-sc to increase the EE formation, and UAS-Dilp3^{RNAi} to deplete the *Dilp3* RNA. Flies approximately 7 days old were transferred to 29°C for 4 days to allow the expression of the transgenes. The flies were then used for gut dissection and p-H3 staining.

Data are presented as mean ± SEM (error bar).

Tk and *Dilp3* mRNA (Figures 4A and 4B), and mitotic count (Figure 4C). The Tk-Gal4-driven expression of another proapoptotic protein, Hid, caused a less efficient killing of EEs (Figure S4J) and subsequently no reduction of p-H3 count (Figure 4C). The knockdown of *Tk* itself by Tk-Gal4 also caused significant reduction of p-H3 count (Figure 4D). A previous report revealed the expression by antibody staining of a Tk receptor (TkR86C) in visceral muscles (Poels et al., 2009), and our knockdown of *TkR86C* in smooth muscle by Dilp3-Gal4 or Mef2-Gal4 showed a modest but significant decrease in ISC proliferation (Figure 4E, F). There was a concomitant reduction of *Dilp3* mRNA in guts of all these experiments (Figures S4K–S4M), while the head *Dilp3* mRNA had no significant change in all these experiments. As a comparison, *TkR99D* or *NPFR* RNAi did not show the same consistent defect.

In conclusion, we show that among the *AS-C* genes, *sc* is the one essential for the formation of all adult midgut EEs and is probably required during metamorphosis when the midgut is reformed. In newly eclosed flies, EEs serve as a link between diet-stimulated *Dilp3* expression in the visceral muscle and ISC proliferation. Depletion of Tk-expressing EEs caused similar *Dilp3* expression and ISC proliferation defects, although the defects appeared to be less severe than that in the *sc* RNAi/EE-less guts. The results together suggest that Tk-expressing EEs are part of the EE population required for this regulatory circuit. The approach we report here has established the *Drosophila* midgut as a model to dissect the function of EEs in intestinal homeostasis and whole-animal physiology.

EXPERIMENTAL PROCEDURES

Drosophila Stocks and Tissue Staining

All *Drosophila* stocks were maintained at room temperature in yeast extract/cornmeal/molasses/agar food medium. UAS-mCD8GFP and w^{1118} were used for crossing with Gal4 and mutant lines as control. The fly stocks ac^{RNAi} (29586), ase^{RNAi} (31895), lsc^{RNAi} (27058), sc^{RNAi} (26206), ato^{RNAi} (26316), Tk^{RNAi} (25800), NPF^{RNAi} (27237), sc^{1}, sc^{3B}, sc^{5}, sc^{6}, ato^{1}, $Df(1)sc^{10-1}$, *Df(3R)p13*, and UAS-sc were obtained from Bloomington Stock Center. $TkR86C^{RNAi}$ (13392), $TkR99D^{RNAi}$ (43329), and $NPFR^{RNAi}$ (107663) were obtained from VDRC. esg-Gal4, $Dilp3^{RNAi}$ (33681), Dilp3-Gal4, Mef2-Gal4, and pros-Gal4 have been described previously (Micchelli and Perrimon, 2006; O'Brien et al., 2011;

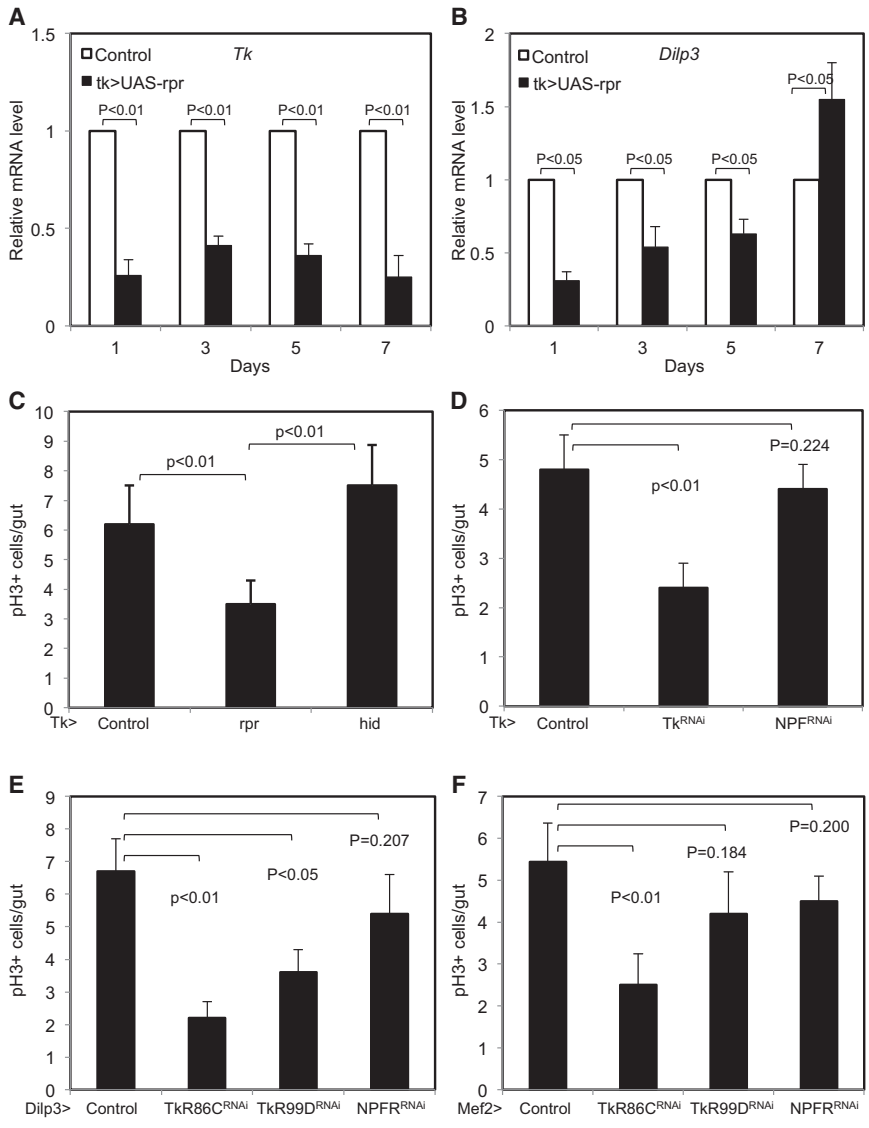

Figure 4. Tk Secreting EEs Have a Role in Regulating Dilp3 and ISC Proliferation

(A and B) Tk-Gal4 flies were crossed with UAS-rpr to induce killing of a subpopulation of EE cells. Tk > GFP was the control. Flies at the indicated days at room temperature after hatch were used for gut dissection and PCR assay. Each PCR cycle number of *Tk* and *Dilp3* was normalized with the cycle number of *rp49* in a parallel reaction of the same RNA sample. The control sample at each time point was set as 1 and UAS-rpr samples were plotted as a fraction of the control.

(C) The same flies at 3 days as above and together with Tk > hid were used to quantify the number p-H3+ mitotic ISCs.

(D) The flies containing the Tk-Gal4 driver were crossed with UAS-RNAi strains for *Tk* and *NPF*. The control was UAS-GFP. Three-day-old progeny flies were dissected for p-H3 staining and quantification.

(E and F) The flies containing the Dilp3-Gal4 or Mef2-Gal4 expressing in visceral muscle were crossed with UAS-RNAi strains for the receptors TkR86C, TkR99D, and NPFR. The control was UAS-GFP. Three-day-old progeny flies were dissected for p-H3 staining and quantification.

Data are presented as mean ± SEM (error bar).

Sen et al., 2004). The Tk-Gal4 line was among a set of *Tk* promoter Gal4 lines screened for expression in the adult midgut, and it contains an approximately 1 kb fragment 2.5 kb upstream of the *Tk* transcription start (Song et al., 2014, in this issue of *Cell Reports*). Female flies were used for routine gut dissection because of the bigger size. Immunofluorescence staining, antibodies used, microscope image acquisition, and processing were as described previously (Amcheslavsky et al., 2009, 2011).

Feeding, Fecundity, and Enzyme Assays

For feeding experiments, newly hatched or appropriately aged flies were kept in regular food vials or in plastic vials with a filter paper soaked with 1% sucrose in water and transferred to fresh vials every day. For dye-ingestion experiments, 20 flies were transferred to a plastic vial with a filter paper soaked with 5% sucrose and 0.5% bromophenol blue sodium salt (B5525, Sigma). At the indicated time, flies that showed visible blue abdomen were counted or used for gut-extract preparation and OD measurement. For defecation experiments, flies were placed in new vials with sucrose/bromophenol blue, and colored excreta on the vial wall were counted at 4 and 24 hr time points. For gut-clearance assays, flies were first fed with bromophenol blue, and ten flies that had blue abdomen were transferred to a new vial containing 5% sucrose only. At 2 and 24 hr after, flies were counted based on whether they still had blue abdomen or not. For fecundity assays, newly hatched male and virgin female flies were aged for 5 days on a normal diet. A group of ten females and five males were put together in a new food vial and transferred to a fresh food vial every day. The number of eggs was counted in each vial for 10 days. Vials were kept to allow larvae and pupae to develop, and the number of pupae was counted for every vial. For digestive enzyme assays, midguts from fertilized females (7–10 days old) were homogenized in 50 μl PBS at 5,000 rpm for 15 s (Precellys 24, Bertin Technologies) and centrifuged (10.000 × *g* for 10 min). Substrates for trypsin enzymatic assay (C8022) were purchased from Sigma-Aldrich, and the reaction was set up following the manufacturer's instructions. Increase in absorbance (405 nm) or fluorescence (355 nm/460 nm) after substrate cleavage was monitored by a microplate reader (Mithras LB 940, Berthold Technologies). Each genotype corresponded to five to six samples of ten midguts each.

Real-Time qPCR

Total RNA was isolated from ten dissected female guts and used to prepare cDNA for quantitative PCR (qPCR) using a Bio-Rad iQ5 System (Amcheslavsky et al., 2011). qPCR was performed in duplicate from each of at least three independent biological samples. The *ribosomal protein 49* (*rp49*) gene expression was used as the internal control for normalization of cycle number. The primer sequences are listed in the Supplemental Experimental Procedures.

All error bars represent SEM, and p values are from the Student's t test.

SUPPLEMENTAL INFORMATION

Supplemental Information includes Supplemental Experimental Procedures and three figures and can be found with this article online at http://dx.doi.org/10.1016/j.celrep.2014.08.052.

AUTHOR CONTRIBUTIONS

A.A., Q.L., Y.N., and Y.T.I. designed, carried out, and analyzed the experiments. W.S. and N.P. performed the experiments that identified the TK-Gal4 gut driver, expression pattern, and cell-killing conditions. I.B. and D.F. designed and performed the gut digestive enzyme and feeding assays. A.A. and Y.T.I. wrote the manuscript. All authors amended the manuscript.

ACKNOWLEDGMENTS

We acknowledge the Vienna Drosophila RNAi Center and the Bloomington Drosophila Stock Center for providing fly stocks. We thank Lucy O'Brien for the kind provision of fly stocks and reagents. Y.T.I. is supported by an NIH grant (DK83450) and is a member of the UMass DERC (DK32520), the UMass Center for Clinical and Translational Science (UL1TR000161), and the Guangdong Innovative Research Team Program (201001Y0104789252). Work in the N.P. laboratory is supported by HHMI and the NIH. Work in the D.F. laboratory was funded by CNRS and ANR Drosogut. I.B. was supported by the Sao Paulo regional government.

Received: July 21, 2013
Revised: March 25, 2014
Accepted: August 21, 2014
Published: September 25, 2014

REFERENCES

Amcheslavsky, A., Jiang, J., and Ip, Y.T. (2009). Tissue damage-induced intestinal stem cell division in Drosophila. Cell Stem Cell *4*, 49–61.

Amcheslavsky, A., Ito, N., Jiang, J., and Ip, Y.T. (2011). Tuberous sclerosis complex and Myc coordinate the growth and division of Drosophila intestinal stem cells. J. Cell Biol. *193*, 695–710.

Bardin, A.J., Perdigoto, C.N., Southall, T.D., Brand, A.H., and Schweisguth, F. (2010). Transcriptional control of stem cell maintenance in the Drosophila intestine. Development *137*, 705–714.

Biteau, B., and Jasper, H. (2011). EGF signaling regulates the proliferation of intestinal stem cells in Drosophila. Development *138*, 1045–1055.

Biteau, B., and Jasper, H. (2014). Slit/Robo signaling regulates cell fate decisions in the intestinal stem cell lineage of Drosophila. Cell Rep *7*, 1867–1875.

Buchon, N., Broderick, N.A., Kuraishi, T., and Lemaitre, B. (2010). Drosophila EGFR pathway coordinates stem cell proliferation and gut remodeling following infection. BMC Biol. *8*, 152.

Cognigni, P., Bailey, A.P., and Miguel-Aliaga, I. (2011). Enteric neurons and systemic signals couple nutritional and reproductive status with intestinal homeostasis. Cell Metab. *13*, 92–104.

Cordero, J.B., Stefanatos, R.K., Scopelliti, A., Vidal, M., and Sansom, O.J. (2012). Inducible progenitor-derived Wingless regulates adult midgut regeneration in Drosophila. EMBO J. *31*, 3901–3917.

Durand, A., Donahue, B., Peignon, G., Letourneur, F., Cagnard, N., Slomianny, C., Perret, C., Shroyer, N.F., and Romagnolo, B. (2012). Functional intestinal stem cells after Paneth cell ablation induced by the loss of transcription factor Math1 (Atoh1). Proc. Natl. Acad. Sci. USA *109*, 8965–8970.

García-Bellido, A., and de Celis, J.F. (2009). The complex tale of the achaete-scute complex: a paradigmatic case in the analysis of gene organization and function during development. Genetics *182*, 631–639.

Gerbe, F., Legraverend, C., and Jay, P. (2012). The intestinal epithelium tuft cells: specification and function. Cell. Mol. Life Sci. *69*, 2907–2917.

Guo, Z., Driver, I., and Ohlstein, B. (2013). Injury-induced BMP signaling negatively regulates Drosophila midgut homeostasis. J. Cell Biol. *201*, 945–961.

Jiang, H., and Edgar, B.A. (2009). EGFR signaling regulates the proliferation of Drosophila adult midgut progenitors. Development *136*, 483–493.

Jiang, H., Patel, P.H., Kohlmaier, A., Grenley, M.O., McEwen, D.G., and Edgar, B.A. (2009). Cytokine/Jak/Stat signaling mediates regeneration and homeostasis in the Drosophila midgut. Cell *137*, 1343–1355.

Jiang, H., Grenley, M.O., Bravo, M.J., Blumhagen, R.Z., and Edgar, B.A. (2011). EGFR/Ras/MAPK signaling mediates adult midgut epithelial homeostasis and regeneration in Drosophila. Cell Stem Cell *8*, 84–95.

Li, H., Qi, Y., and Jasper, H. (2013a). Dpp signaling determines regional stem cell identity in the regenerating adult Drosophila gastrointestinal tract. Cell Rep *4*, 10–18.

Li, Z., Zhang, Y., Han, L., Shi, L., and Lin, X. (2013b). Trachea-derived dpp controls adult midgut homeostasis in Drosophila. Dev. Cell *24*, 133–143.

Lin, G., Xu, N., and Xi, R. (2008). Paracrine Wingless signalling controls self-renewal of Drosophila intestinal stem cells. Nature *455*, 1119–1123.

Micchelli, C.A., and Perrimon, N. (2006). Evidence that stem cells reside in the adult Drosophila midgut epithelium. Nature *439*, 475–479.

Micchelli, C.A., Sudmeier, L., Perrimon, N., Tang, S., and Beehler-Evans, R. (2011). Identification of adult midgut precursors in Drosophila. Gene Expr. Patterns *11*, 12–21.

Miguel-Aliaga, I. (2012). Nerveless and gutsy: intestinal nutrient sensing from invertebrates to humans. Semin. Cell Dev. Biol. *23*, 614–620.

O'Brien, L.E., Soliman, S.S., Li, X., and Bilder, D. (2011). Altered modes of stem cell division drive adaptive intestinal growth. Cell *147*, 603–614.

Ohlstein, B., and Spradling, A. (2006). The adult Drosophila posterior midgut is maintained by pluripotent stem cells. Nature *439*, 470–474.

Osman, D., Buchon, N., Chakrabarti, S., Huang, Y.T., Su, W.C., Poidevin, M., Tsai, Y.C., and Lemaitre, B. (2012). Autocrine and paracrine unpaired signaling regulate intestinal stem cell maintenance and division. J. Cell Sci. *125*, 5944–5949.

Poels, J., Birse, R.T., Nachman, R.J., Fichna, J., Janecka, A., Vanden Broeck, J., and Nässel, D.R. (2009). Characterization and distribution of NKD, a receptor for Drosophila tachykinin-related peptide 6. Peptides *30*, 545–556.

Reeves, N., and Posakony, J.W. (2005). Genetic programs activated by proneural proteins in the developing Drosophila PNS. Dev. Cell *8*, 413–425.

Sato, T., van Es, J.H., Snippert, H.J., Stange, D.E., Vries, R.G., van den Born, M., Barker, N., Shroyer, N.F., van de Wetering, M., and Clevers, H. (2011). Paneth cells constitute the niche for Lgr5 stem cells in intestinal crypts. Nature *469*, 415–418.

Scopelliti, A., Cordero, J.B., Diao, F., Strathdee, K., White, B.H., Sansom, O.J., and Vidal, M. (2014). Local control of intestinal stem cell homeostasis by enteroendocrine cells in the adult Drosophila midgut. Curr. Biol. *24*, 1199–1211.

Sen, A., Kuruvilla, D., Pinto, L., Sarin, A., and Rodrigues, V. (2004). Programmed cell death and context dependent activation of the EGF pathway regulate gliogenesis in the Drosophila olfactory system. Mech. Dev. *121*, 65–78.

Song, W., Veenstra, J.A., and Perrimon, N. (2014). Control of lipid metabolism by tachykinin in Drosophilia. Cell Reports *9*, this issue, 40–47.

Takashima, S., Adams, K.L., Ortiz, P.A., Ying, C.T., Moridzadeh, R., Younossi-Hartenstein, A., and Hartenstein, V. (2011). Development of the Drosophila entero-endocrine lineage and its specification by the Notch signaling pathway. Dev. Biol. *353*, 161–172.

Tian, A., and Jiang, J. (2014). Intestinal epithelium-derived BMP controls stem cell self-renewal in Drosophila adult midgut. Elife *3*, e01857.

VanDussen, K.L., and Samuelson, L.C. (2010). Mouse atonal homolog 1 directs intestinal progenitors to secretory cell rather than absorptive cell fate. Dev. Biol. *346*, 215–223.

Veenstra, J.A., Agricola, H.J., and Sellami, A. (2008). Regulatory peptides in fruit fly midgut. Cell Tissue Res. *334*, 499–516.

Xu, N., Wang, S.Q., Tan, D., Gao, Y., Lin, G., and Xi, R. (2011). EGFR, Wingless and JAK/STAT signaling cooperatively maintain Drosophila intestinal stem cells. Dev. Biol. *354*, 31–43.

Zeng, X., Lin, X., and Hou, S.X. (2013). The Osa-containing SWI/SNF chromatin-remodeling complex regulates stem cell commitment in the adult Drosophila intestine. Development *140*, 3532–3540.

Zhou, F., Rasmussen, A., Lee, S., and Agaisse, H. (2013). The UPD3 cytokine couples environmental challenge and intestinal stem cell division through modulation of JAK/STAT signaling in the stem cell microenvironment. Dev. Biol. *373*, 383–393.

Cell Reports, Volume *9*

Supplemental Information

Enteroendocrine Cells Support Intestinal Stem-Cell-Mediated Homeostasis in *Drosophila*

Alla Amcheslavsky, Wei Song, Qi Li, Yingchao Nie, Ivan Bragatto, Dominique Ferrandon, Norbert Perrimon, and Y. Tony Ip

Figure S1. Related to main text Figure 1A-B.

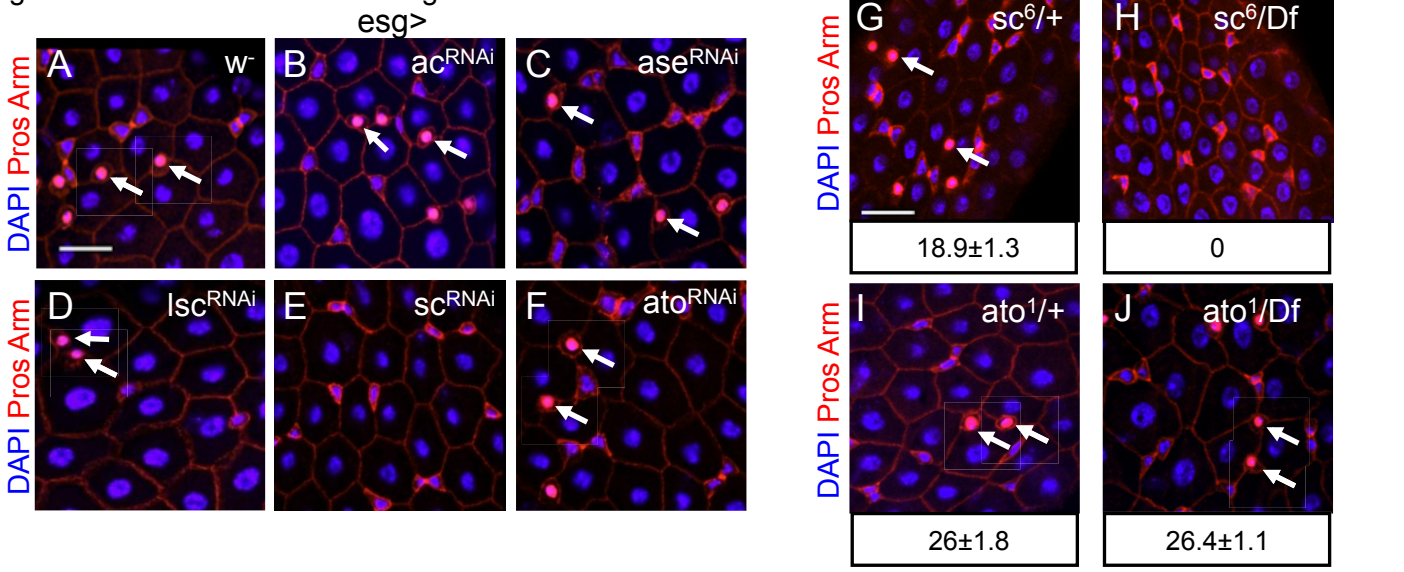

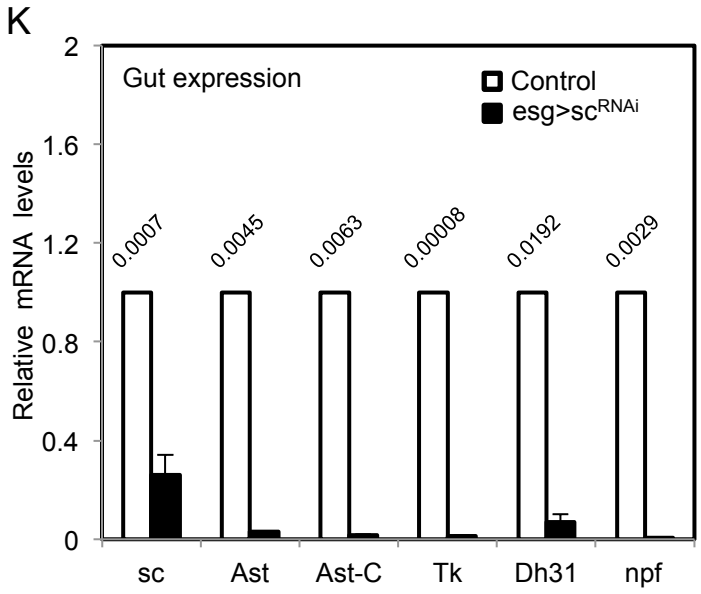

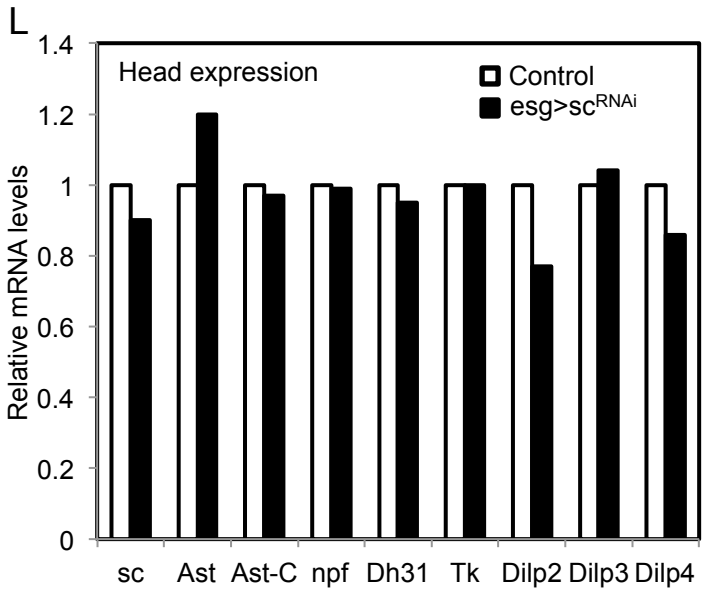

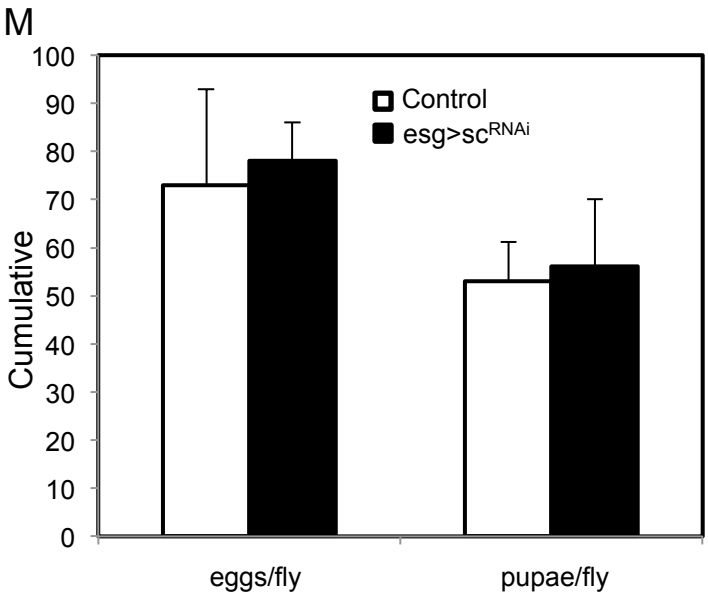

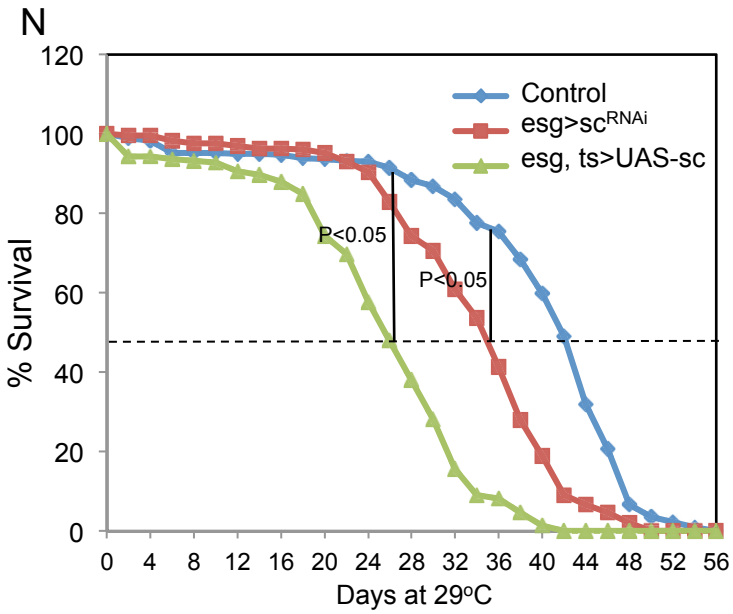

Figure S1. EE number, hormone gene expression and life span after loss of *sc* function. (A-F) Confocal images of adult midgut surface views. esg-Gal4 flies were crossed with *w-* or the indicated UAS-RNAi constructs. 7 days old flies were used for dissection and staining. For all images in this figure, blue is DAPI for DNA, red membrane is Armadillo (β-catenin) and red nuclear is Prospero. The arrows point to examples of EEs. Scale bar is 20 μm. (G-J) Confocal images from the midguts of flies with the indicated genotypes. The deficiency for *sc* was *Df(1)sc*$^{10-1}$ and for *ato* was *Df(3R)p13*. (K, L) Peptide hormone gene expression in midgut and head. 5 days old flies were used for dissection and RNA isolation from heads and midguts. The cycle number of each gene was normalized with that of *rp49* in a parallel reaction of the same RNA sample. The level of expression relative to *rp49* in control sample is shown at the top of each white bar, and this normalized expression was set as 1 for each gene. The expression of that gene in the *sc*^{RNAi} guts was calculated as the ratio to that in control. (M) For fecundity assay, males and females were put together and transferred to new vials every day. Eggs were counted in each vial for 10 days. Four independent experiments were performed and the average cumulative number of eggs laid per female fly was plotted. After flies were transferred out, the vials were kept and the embryos were let grown and the pupae were counted. Four independent experiments were performed and the average pupae number per female fly was plotted. (N) 100 flies of each genotype were kept at 29^{o}C in normal food vials and transferred to fresh vials every other day. The percent of flies survived at each time was recorded. The experiment was performed 3 times, and the average at each time point was plotted. The P value was calculated by comparing the survival of control sample on the same day as 50% survival of the *sc* samples.

Figure S2. Related to main text Figure 1C-H.

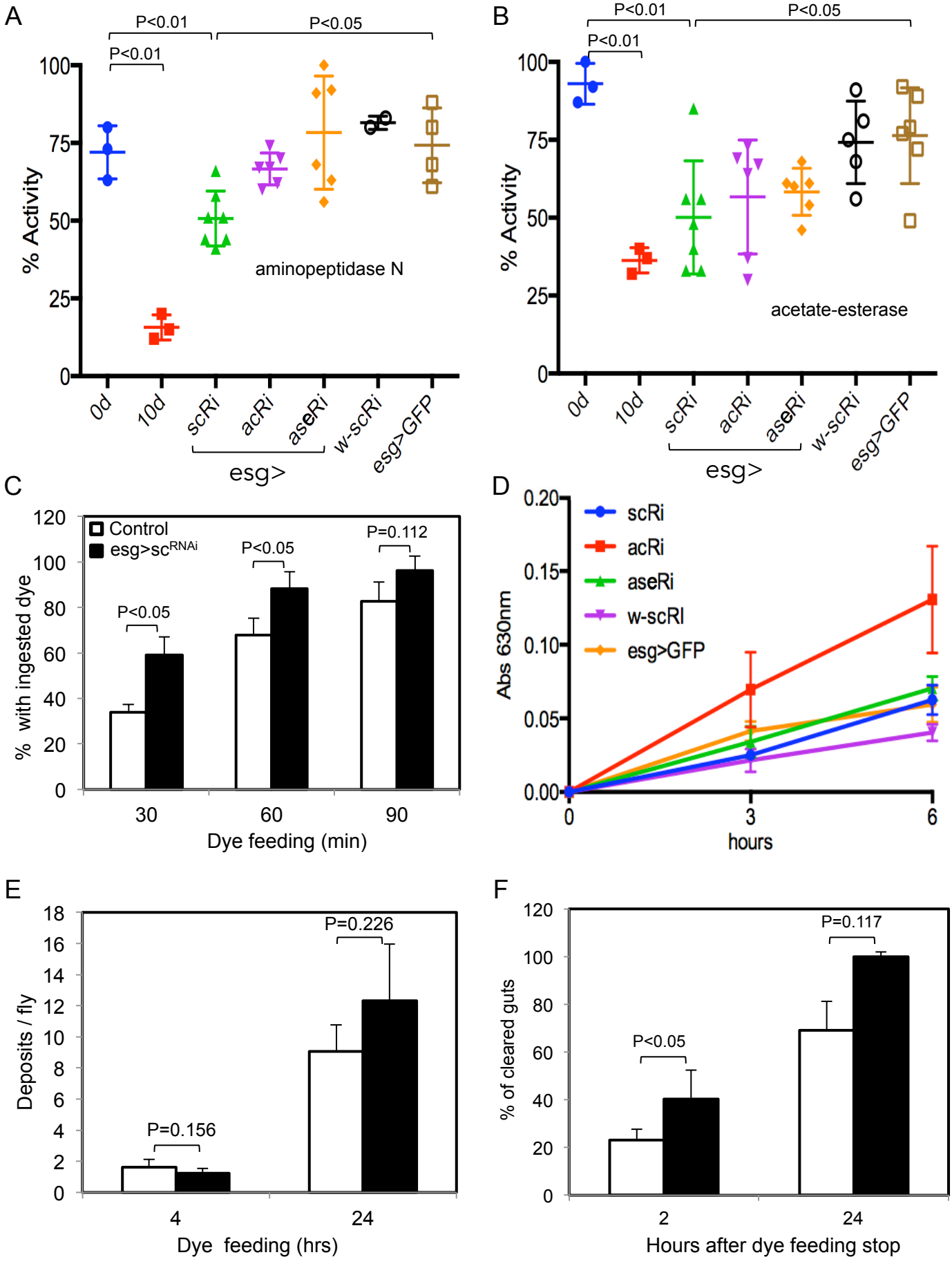

Figure S2. Digestive enzyme activities, food intake and food passage assays in EE-less flies. (A-B) For digestive enzyme assay, midguts from 7 days old females were homogenized and mixed with the corresponding substrate for the indicated enzymatic assay. Each genotype analyzed had 5-6 samples of 10 midguts each. (C) 20 control and esg>sc^{RNAi} flies were transferred to plastic vials containing a filter paper soaked with 5% sucrose in water and 0.5% bromophenol blue (BPB) sodium salt. Every 30 minutes flies that had visible ingested dye in the abdomen were counted. Six independent experiments were performed and the average accumulative at each time point was plotted. (D) 10 midguts from 7 days old females of each genotype were pooled at 3 and 6 h after transferring the flies to a plastic vial containing a solution of sucrose 50 mM (1.71%) and 2.5% (w/v) blue dye (food colorant E131). Food intake was monitored by the increase in absorbance at 630 nm (Mithras LB 940, Berthold Technologies) of the supernatant after midgut homogenization and centrifugation (10.000x g 10 min). Average of 3 experiments was plotted. (E-F) The fly strains were kept in 5% sucrose and 0.5% BPB. At the indicated times, blue deposits on the plastic vials were counted. Similarly, 10 flies were well fed to have visible blue abdomens and then transferred to a new vial containing 5% sucrose solution. Flies that had clear abdomens were counted after the time as indicated. Three independent experiments were performed and the average was plotted.

Figure S3. Related to main text Figure 3.

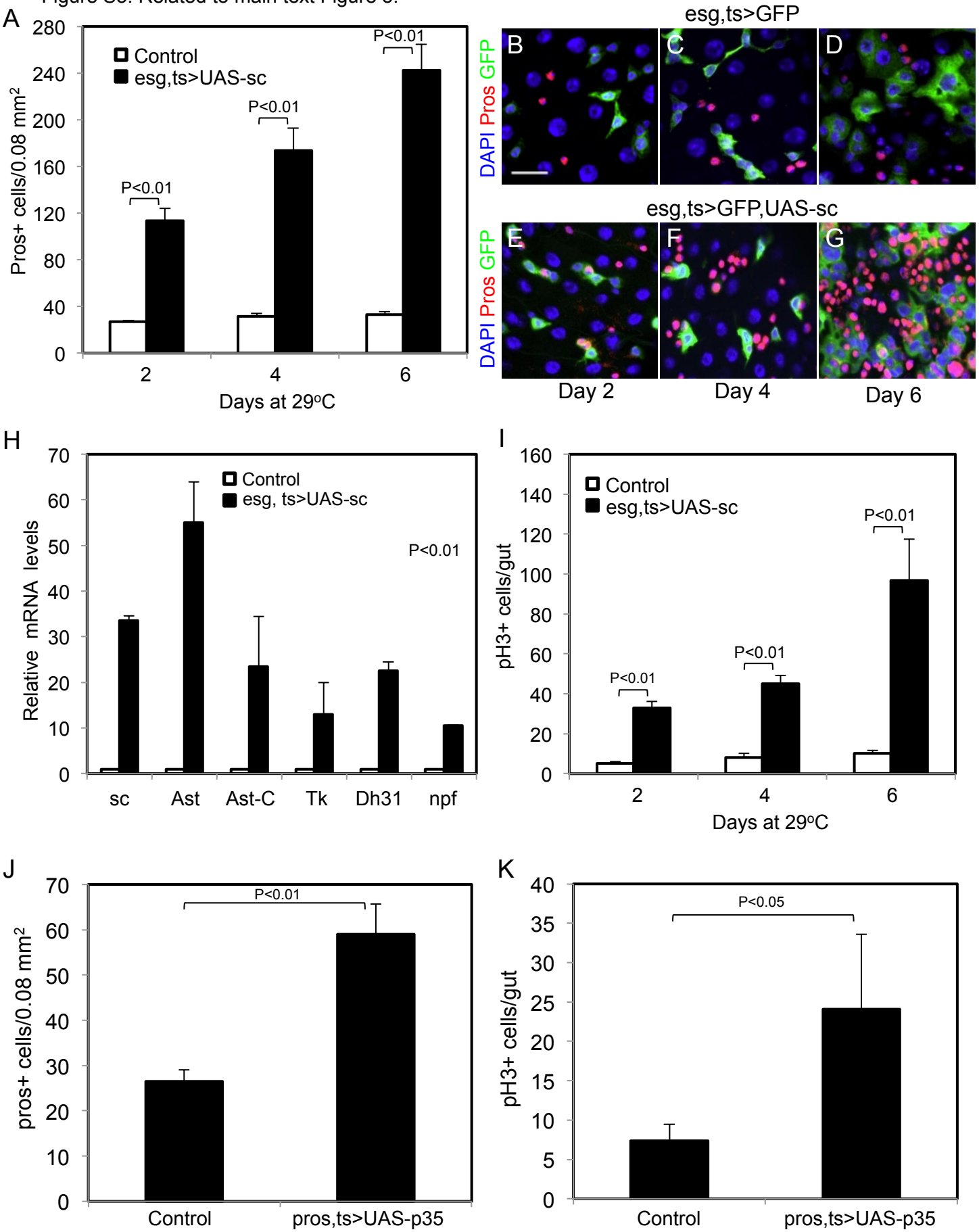

Figure S3. EE number correlates with ISC proliferation. (A) The flies approximately 7 days old were shifted to 29°C for 2 to 6 days to inactivate Gal80^{ts} and allow Gal4 to activate UAS-*sc* expression. Quantification of Prospero+ nuclei were performed from midguts of esg^{ts}>GFP control and esg^{ts}>GFP, UAS-*sc* flies. (B-G) Representative confocal images of midgut surface views from control and *sc* over-expression flies. Blue is DAPI for DNA, red nuclear is Prospero and green is mCD8GFP. The scale bar is 20 μm. (H) The esg^{ts}>GFP control and the esg^{ts}>GFP, UAS-*sc* flies were shifted to 29°C for 4 days and used for gut dissection and RNA isolation. The primer sets for the indicated genes were used for qPCR. The cycle number of each gene was normalized with that of *rp49* in a parallel reaction of the same RNA sample. The normalized expression of each gene in the control sample was set as 1 and the expression of that gene in the UAS-*sc* background was calculated as fold change. (I) Average number of p-H3+ cells in whole midguts of esg^{ts}>GFP control and esg^{ts}>GFP, UAS-sc flies. 7 days old flies were shifted to 29°C to initiate *sc* overexpression. At the days indicated, a portion of the flies was used for midgut dissection and p-H3 staining. (J-K) The *pros* promoter-Gal4 and tubulinGal80^{ts} (pros^{ts}>)were crossed with UAS-GFP control and UAS-p35 transgenic flies. 5 days old flies were shifted to 29°C for 4 days and then used for gut dissection, Pros and p-H3 staining, and quantification.

Figure S4. Related to main text Figure 4.

A

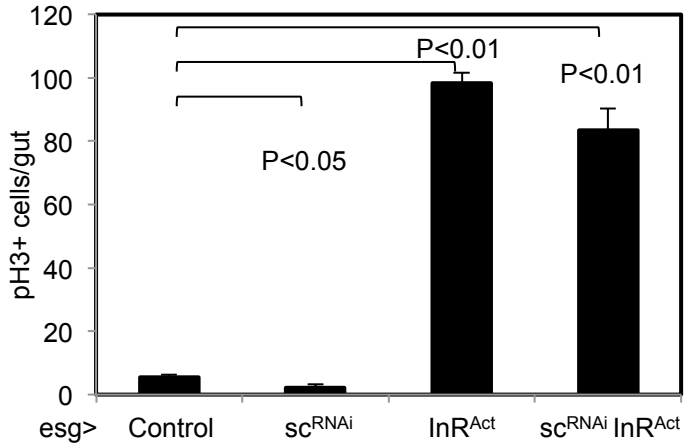

B

	% Gal4+ cells that are EEs	% EEs that are Gal4+
	Pros+/prosGal4>GFP+(%)	ProsGal4>GFP+/Pros+ (%)
Middle Midgut	100 +/- 0	88 +/- 7.7
Posterior Midgut	69 +/- 13	35 +/- 6.9
	Pros+/TkGal4>GFP+ (%)	TkGal4>GFP+/Pros+ (%)
Middle Midgut	100 +/- 0	12 +/- 6.4
Posterior Midgut	100 +/- 0	61 +/- 4.3

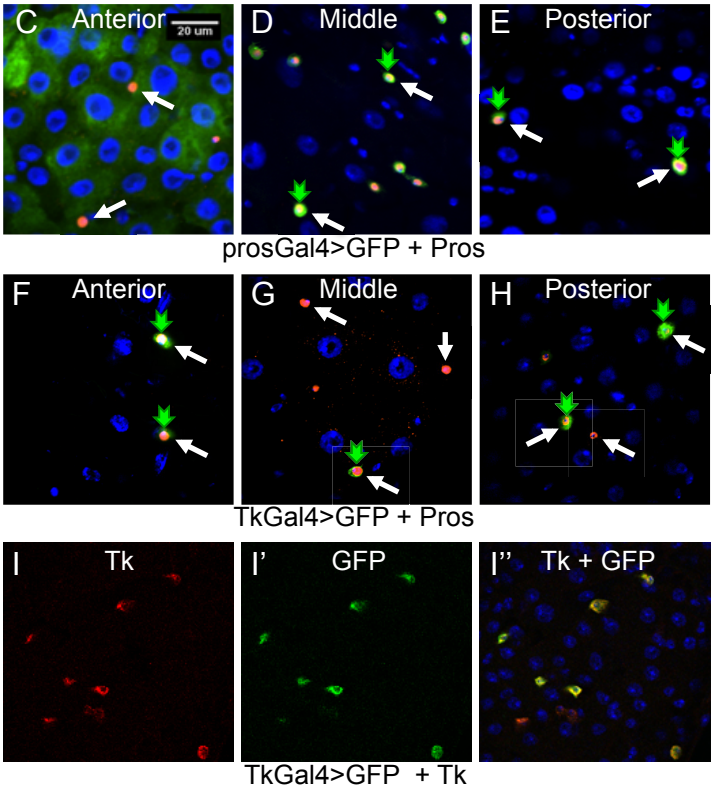

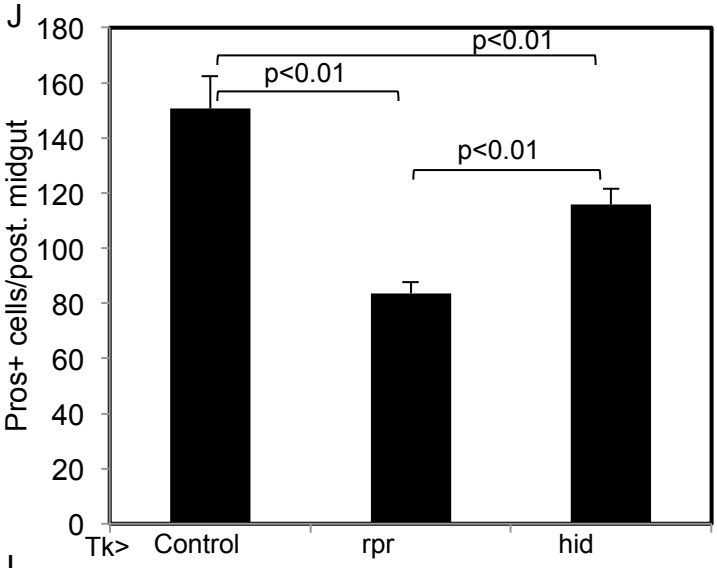

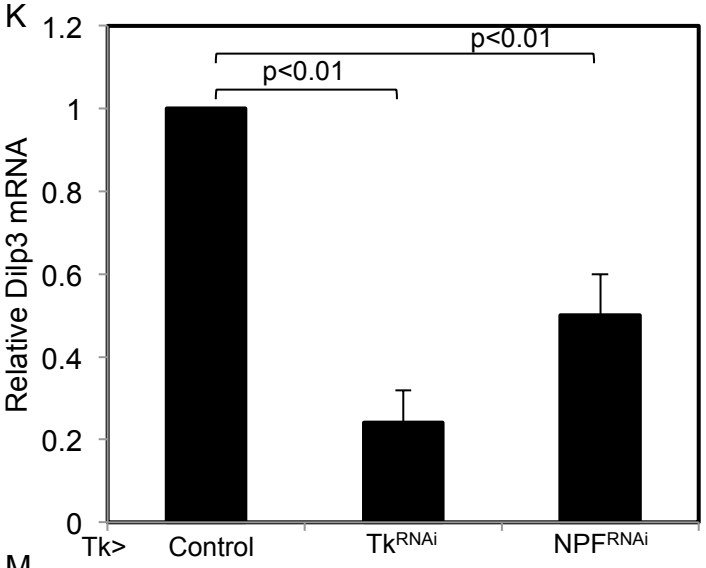

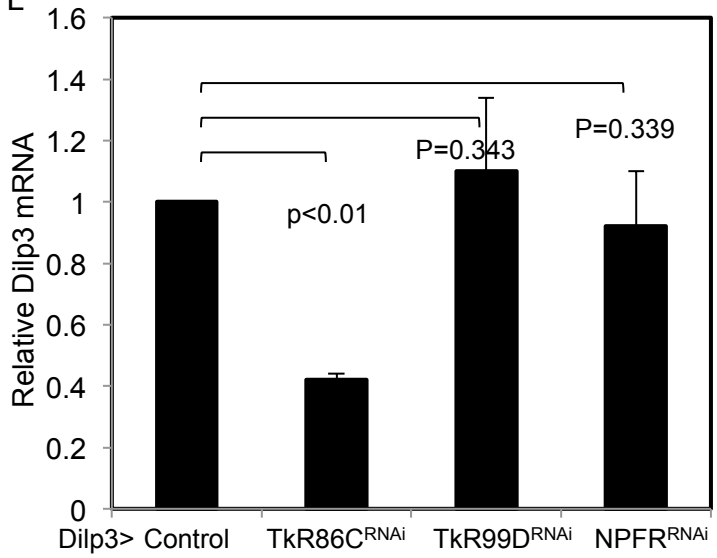

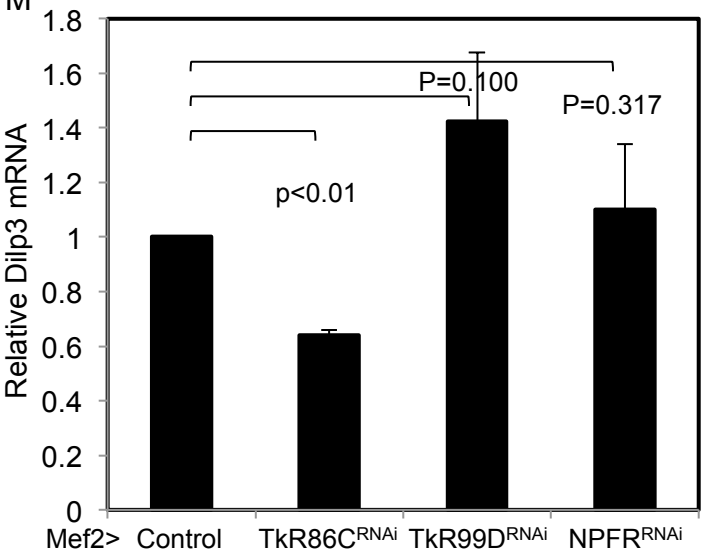

Figure S4. Midgut expression of pros-Gal4 and Tk-Gal4 and functional assays of TK signaling. (A) The esg-Gal4 was used to express an activated insulin receptor (InR^{Act}), together with the scRNAi. Flies 3 days after eclosion were used for gut dissection and p-H3 quantification. (B) Quantification of Pros+ staining overlapping with the Gal4 driven GFP+ cells. The ratios are calculated to show the percentage of GFP+ cells that should be EEs, or to show the percentage of EEs that have the Gal4>GFP expression. (C-I'') UAS-GFP were crossed with the Gal4 drivers as indicated and midguts of 5-7 days old flies were dissected and stained using antibodies for Pros (C-H) or Tk (I-I'') proteins. The arrows indicate examples of Pros+ nuclear staining, and the wide green arrows indicate overlapping GFP+ staining in some EEs. The GFP signal in panel C reveals pros-Gal4 expression in the ECs of a small anterior midgut region. Although we did not observe obvious increase of p-H3+ cells in this anterior region from the pros-Gal4/UAS-p35 experiments, we counted p-H3 staining from middle and posterior midguts only for these experiments. (J) The same experiments as in Fig. 4C, and the guts were stained and quantified for Pros+ EEs. (K) The same experiments as in Fig. 4D, and the guts were used for PCR quantification of *Dilp3* mRNA. (L, M) The same experiments as in Fig. 4E and F, and the guts were used for PCR quantification of *Dilp3* mRNA.

qPCR primer sequences. Related to Real-time qPCR in Experimental Procedures.

scute: 5'-CAATTCGGCAACGAAGAT and 5'-CAGCGGGTTGATTTTGAT

allatostatin: 5'-TCCGCAACCCTTCAACTT and 5'- TGAATAAGTGCGCCATCC

allatostatin C: 5'-AGTTAACGCGACCAAAGG and 5'-AGTTTTTCGGCCTTGATG

neuropeptide F: 5'-ACCATGGCAACGTCACTA and 5'-AACTATTGCCCCGAAAAA

diuretic hormone: 5'-CAAACGAACCGTGGACTT and 5'-CAGACCCATGCGATGTTT

tachykinin: 5'-TACGCGAGCATTTGGACA and 5'-GAAATCGATGCGCTGAAG

phyllopod: 5'-CCTCCTCGGAATACCTGAAAC and 5'-GCCTGGATTAGCTGAACGATA

Dilp2: 5'-ATGGTGTGCGAGTATAATCC and 5'-TCGGCACCGGGCATG

Dilp3: 5'-AGAGAACTTTGGACCCCGTGAA and 5'-TGAACCGAACTATCACTCAACAGTCT

Dilp4: 5'-GCGGAGCAGTCGTCTAAGGA and 5'-TCATCCGGCTGCTGTAGCTT

rp49: 5'-CGGATCGATATGCTAAGCTGT and 5'-GCGCTTGTTCGATCCGTA